EXPERIMENTAL APPROACH TO THE HYDRAULICS OF VERTICAL SLOT FISHWAYS

By J. PUERTAS[1], Aff. Member, ASCE, L. PENA[2], T. TEIJEIRO[3]

https://ascelibrary.org/doi/10.1061/%28ASCE%290733-9429%282004%29130%3A1%2810%29Abstract:

Fishways are hydraulic structures that enable fish to go through transverse obstructions to continue their upstream migrations. This paper presents the results of a scale model of a vertical slot fishway. The performance of two particular designs of vertical slot fishways for two different slopes was studied in a wide range of discharges. Water depths were measured in almost the whole surface of pools. A linear relation between dimensionless discharge and depth of flow, and the same flow patterns for each design were found. With an acoustic Doppler velocimeter (ADV), three-dimensional velocities were measured at several levels in the entire pool to detect the structure of the flow and quantify velocity distribution. Two different regions in flow patterns were found: a direct flow region characterized by maximum velocities; and a recirculation region, defined by low velocities and horizontal eddies. For a given slope, the velocity at any point of the pool (particularly at the slot) may be considered independent of the discharge and constant with the depth. Some suggestions on kinetic turbulent energy are also made.

INTRODUCTION

Fish populations in rivers are highly dependent on the characteristics of their aquatic habitat, since it provides the support for all their biological functions. This dependency is more critical in the case of migratory fish which require different habitats to complete their life cycle (Larinier *et al.* 1998). Anadromous fish species (Salmonidae, Clupeidae, Petromyzontidae...) have to overcome several obstacles in their migration upstream which may prevent their free ascension to the spawning areas. These obstructions, which can be of natural origin (gorges, rapids, waterfalls) or man-made (usually hydraulics works of different types: dams, barriers, watermills...), prevent, as a direct consequence, the natural migrations of fish up and in some cases downstream. This restriction of the "free circulation" of fish is known as the barrier effect, which makes it impossible for the migratory fish to complete their life cycle. It also isolates and separates fish population, drastically diminishing the number of local species. Fish passage structures and vertical slot fishways in particular try to minimize the

[1] Prof., Civil Engineering School, A Coruña University, Campus de Elviña, s/n, 15912, A Coruña, Tel: (+34)981 167000 Ext. 5185, Fax: (+34) 981167179, E-mail: puertas@iccp.udc.es

[2] Res., CITEEC, A Coruña University, Campus de Elviña, s/n, 15912, A Coruña, Tel: (+34)981 167000 Ext. 5185, Fax: (+34) 981167179, E-mail: citeec7@mail2.udc.es

[3] Prof., EPS, Santiago de Compostela University, Bernardino Pardo Ouro, s/n, 27002, Lugo, Tel: (+ 34) 982 223 325 Ext 23250, Fax: (+ 34) 982 241 835, E-mail: ttreps@usc.lugo.es

negative effects caused by transverse hydraulics constructions and to facilitate the exploitation of species over a wider extension (Larinier *et al*. 1999). For any fishway to be considered effective, it must allow fish to easy access to the fishway inlet, as well as letting fish go through the fishway with no delay, stress or injury, so that they can head for their spawning areas in a natural way.

Although biological and hydraulic aspects are essential to developing a good design of a specific fishway and, therefore, being able to minimize negative impacts on migratory river fauna, it must be remembered that all damages that might be caused by an obstacle can never be fully compensated by fishways.

The earliest vertical slot fishways was developed by Milo C. Bell and built at the Hell´s Gate on Fraser River, Canada (Clay, C.H. 1995). A vertical slot fishway consists of a rectangular channel with a sloping bed divided by baffles into a number of pools. Water travels down the channel through vertical slots, passing from one pool to the next one below (Wu *et al.*, 1999) until it finally reaches the river past the obstacle. The difference in water level between the upper and lower end of the fishway is divided into a number of small falls (Rajaratnam *et al*. 1986). Water flows through the slot like a jet and its energy becomes dissipated by the mixing of the jet in the pool.

Fishways must attract fish towards the inlet and let them ascend, so that the water velocity in the flume must not overcome the fish burst speed (Beach, B.H., 1984). Vertical slot fishway must also provide resting zones in the pools for the migratory fish so that they may recover their swimming ability after this great exertion. Vertical slot fishways are widely used in small dams (<5 m.) and natural obstructions where discharges are uncontrollable or undergo great variations. The overwhelming advantage of vertical slot fishways is their adaptability to variations in water levels while their hydraulic performance remains stable.

A study of hydraulic characteristics of vertical slot fishways in laboratory model was performed. At the same time, not included here, a numerical simulation of the flow was conducted using the experimental data obtained to calibrate a significant model based on the Finite Volume Method, including turbulence terms.

Previous experimental research on the hydraulics of vertical slot fishways was taken into account. In the research project carried out at the University of Alberta (Canada) by Rajaratnam *et al.* (1986, 1992, 1999) 18 different designs were studied for the following range of slopes S_o=5, 10 and 15%. In all of them it was found a linear relationship between dimensionless discharge Q^* and a relative flow depth y_o/b_o existed, where Q^* was defined as $Q^* = Q/\sqrt{gS_o b_o^5}$, Q being the discharge of the fishway, S_o the geometrical slope of the fishway and b_o the slot width; y_o is the average depth of flow measured at the center of the pools. Taking into account hydraulic criteria such as turbulence levels, the circulation patterns in the pool, the jet velocities and energy dissipation and some other factors like simplicity of design or financial cost, they concluded that for $8b_o$ wide and $10b_o$ long pool designs, the fishway performance was satisfactory. On the basis of the designs studied, Rajaratnam *et al.* (1992) recommended designs 6, 16 and 18 for practical use (Fig. 1). The recommendations of Larinier *et al.* (1998) for pool dimensions also entail a length of 8-10b and a width of 6-8b, and are very similar to the ones proposed by Rajaratnam *et al.* (1992). Wu *et al.* (1999) went further in the study of design 18, and concluded that for a slope of 5%, the main flow travels from one slot to the next through the pool as a 2D curved jet with two recirculation regions, one on each side. For slopes of 10% and 20% the main flow is 3D. The flow at the slot was not perpendicular to the slot. The maximum velocity at the slot was approximately equal to $\sqrt{2g\Delta h}$.

This paper, in an attempt to continue the line of the research begun by Wu *et al.* (1999) on the detailed study of the designs recommended as effective by Rajaratnam *et al.* (1992), focuses on an experimental hydraulic characterization of a scale model of the other two particular vertical slot fishway designs: the so-called design T1 (similar to design 16) and design T2 (similar to design 6). Slight changes were made in their construction in order to adapt them to the existing facilities at the hydraulic research laboratory. The configurations and dimensions of pools are shown in Fig. 2b and Fig. 2c.

To study flow patterns for both design, an experimental program was planned and a detailed study of depth and velocity fields was conduced, since these are the two most important parameters on the hydraulic performance of vertical slot fishway. The relationship between the discharge and the depth is the main factor used to determine the hydraulic performance of the fishway. Depth patterns are important in establishing the water distribution in pools to ensure a minimum water level, enough to allow the passage of the species in question, as well as in adopting design criteria for the fishway height. In addition, the velocity value must be compatible with swimming capabilities of the species concerned and it should determine low velocity flow zones and critical zones which fish will require burst speed (Beach, M.H. 1984).

EXPERIMENTAL ARRANGEMENT

The experimental work was carried out at the CITEEC (Centro de Innovación Tecnolóxica en Edificación e Enxeñería Civil) at the Universidade da Coruña (Spain). The fishway scale model consisted of a metallic structure 12 m long with a 1x1 m^2 rectangular section. The fishway scale model was constructed in such a way as to be able to adopt different slopes. The fishway was divided into eleven pools: a head tank receiving the water from an upstream reservoir, nine active pools and a tailtank. The first four pools presented a T2 configuration, the next were transition type pools and the last four pools had a T1 configuration. The flume bed, side walls and the baffles separating the pools were made of transparent plexiglass sheets (1 cm thick) making it possible to observe the flow. Baffles were always vertical, despite of the slope in the fishway model. The experimental measurements were recorded in pools number 3 and 7 (Fig. 2a). Water was supplied by a hydraulic closed circuit. Discharges was measured by means of an electromagnetic flowmeter. All the elements in the hydraulic circuit were automated and their operation was centralized in a control computer.

Three variables were defined for the arrangement of the experimental study: fishway slope, discharge, and boundary condition. The slopes most frequently used at these types of structures vary between 5-10% (Clay, C.H. 1995 and Larinier *et al.* 1998), hence it was decided to evaluate the fishway for two of them, the first near the lower limit, (S_o=5,7%) and the second, in the vicinity of the upper limit (S_o=10,054%).

The slope value and physical dimensions of the pools determine the limits of discharge range that the model is able to assume; the maximum discharge employed was 125 l/s, for a slope of S_o=10,054%. The minimum discharge providing enough water depth for the functioning of the measurement instruments was set close to 15 l/s and 35 l/s for S_o= 5,7% and S_o=10,054% respectively. Test discharges differed approximately by 10 l/s between them.

A conceptual state of uniform flow (Rajaratnam *et al*. 1986, 1992) was used, so that the mean depth measured at the middle transverse section was the same in all the pools. At the lower end of the flume a tailgate, causing overflow was used to reach the necessary boundary conditions for the uniform flow in each discharge-slope relationship.

A cartesian positioner was placed over the experimental pools in order to automate the positioning of the measurement instruments (Fig. 3). The MAC (Multiuse Axis Control) runs the movement of the electric motors (one on each cartesian axis, X and Y) which draw the supporting metallic beam on which the measurement instruments are fixed. This supporting beam can also be drawn vertically (axis Z). The measurement instruments can, therefore, be set automatically at any point in the pool (3D mesh). Two measurement devices were placed on the cartesian positioner, but not simultaneously: a depth probe and ADV velocimeter.

Velocities were measured by means of a Doppler effect velocimeter (MicroAcoustic Doppler Velocimeter SonTek). The MicroADV is a remote sensing device which has the advantage of being inherently drift-free and does not require routine recalibration. The probe is submerged in the flow and the receivers are slanted at 30º from the axis of the transmit transducer and focus on a common sampling volume, for a total measurement volume of 0.08 cm^3 . The volume is located at 5 cm from the probe to reduce flow interference. The maximum MicroADV sampling rate is 50 Hz. Through the MicroADV Data Acquisition System the specific velocity for the three cartesian axis (V_x,V_y,V_z) was obtained for each data point (Kraus *et al*. 1994; Nikora *et al*. 1998).

Velocity measurements were carried out in planes parallel to the flume bed with 10 cm in between, starting at 5 cm from the channel bed up to as close as possible to the water surface. In each plane, data points were distributed forming a 10x10 cm mesh, reduced to 5x5 cm in critical zones. Therefore a three-dimensional mesh of 10x10x10 cm for the measurement of velocity was maintained. An example of the mesh in one of the planes parallel to the bed for a T1 configurations is shown in Fig. 2d.

Water surface height in the pools was measured by means of a conductivity-based depth probe, DHI Wave Gauge Type 202. The DHI Wave Gauge is comprised of two thin parallel stainless steel electrodes. A conditioning signal module (DHI Wave Meter Conditioning Module Type 102E) receives, processes and amplifies the electric sign sent by the wave gauge. Depth measurements in the pools were evaluated following a bidimensional mesh with data points at a 10x10 cm maximum separation in between. Calibration tests were performed prior to each working day.

A summary of experimental measurements is shown in Table 1. It must be taken into account that the number of measurement planes for the velocity field are variable, thus in the T1 configuration with a slope of 5,7% and a discharge of 35 l/s, 3 planes parallel to the bed were measured; while in the T1 configuration with a slope of 10,054% and a discharge of 125 l/s, 6 planes parallel to the bed were measured.

After a previous experimental tests, a measurement frequency of 15 Hz was chosen. The instrument stayed at each data point for 10 and 15 seconds to collect data on depth and velocity, respectively. Data storage was carried out by a data acquisition program (VirtualBench-Logger, National Instruments). Considering an average of 4 planes parallel to the bed with an average of 132 data points of velocity in each plane (1 data point=675 single data of velocity), 356400 velocity data for each discharge of a given slope and type were measured, all of which provided a large amount of collected data.

ANALYSIS OF THE EXPERIMENTAL RESULTS

The first relationship to be analyzed is the one between dimensionless discharge and depth. Subsequently, some of the relationships between the different characteristic depths (maximum, minimum, mean, at the slot) are shown, as well as depth

distribution at the surface of the pool and in some longitudinal vertical sections. As a consequence, each individual pattern for every configuration should be known, as well as the effects of th slope and discharge on the depth distribution.

When analyzing velocity fields, the distribution of the water velocity has been represented over planes parallel to the bed in order to characterize the different regions into which the velocity field can be divided: recirculation regions and direct flow region. Later, the vertical distributions of velocity values are displayed in order to evaluate their dependence on discharge and velocity. A specific study of the velocity at the slot was done to understand the limitation that this velocity imposes on the design of vertical slot fishways, as these values will be compared with swimming ability of fish.

The passage of migratory fish through the fishway is directly related to the turbulence and aeration in pools. The global energy dissipation per volume unit was used traditionally as an indicator of the turbulence levels in the pools. Also presented is the turbulent kinetic energy from the experimental velocity measurements.

For the representation of the experimental results, the following dimensionless variables were chosen: S_o, geometric slope of the fishway, Y_o/b, relative flow depth at the transverse middle section, Q^A, dimensionless discharge. In previous studies the following dimensionless discharges were proposed:

Rajaratnam *et al*. (1986) $$Q^* = Q \Big/ \sqrt{g S_o b_o^5} \qquad [1]$$

Kamula (2001) $$Q^{**} = Q \Big/ \sqrt{g\, S_o b_o^2 L^3} \qquad [2]$$

where Q^* and Q^{**} are dimensionless discharges, and L is the pool length. It was considered important not to make the dimensionless discharge dependent on the fishway slope in order to detect the individual performance of the fishway for each slope. On the other hand, if the characteristic length L remains invariable (L=1.2 m) for all the designs in our tests, there is no point in including it in the dimensionless parameters. Hence, a new definition for the dimensionless discharge is proposed:

Present Data $$Q^A = Q \Big/ \sqrt{g\, b^5} \qquad [3]$$

Due to its utility, the dimensionless Q^* was used to make the overall comparison of the results obtained in the different designs and for the different slopes including these data and those ofRajaratnam *et al.* (1992). It must be taken into account that the characteristic length of the slot b_o was used by Rajaratnam *et al.* (1986,1992) in some cases, to define the real width of the slot and in other cases, merely a reference width. In this study b has always been set to the real width of the slot (Fig. 1 and Fig. 2).

A summary of the most significant data from the experiments performed is givern in Table 2, where, Y_b is the depth at the slot and Y_m is the average depth in the pool, being Y_{max} and Y_{min} being the maximum and minimum depth in the pool

respectively (all the depth measures represent the vertical distance between the bed and the water free surface). V_b is the velocity at slot, $C_d = Q/(bY_bV_b)$ is a discharge coefficient which is provided to permit a comparison with those given by Rajaratnam *et al.* (1992) and $E = (\rho g Q S_o)/(LWY_0)$ is the energy dissipation rate in the pool.

DEPTH-DISCHARGE EQUATION

Following the indications by Rajaratnam *et al.* (1986), a simple analysis was carried out to determine the flow equations which establish the relationship between the discharge and the depth:

$$Q^A = \alpha\left(\frac{Y_0}{b}\right)^{\lambda} \qquad [4]$$

where $Q^A = Q/\sqrt{g\,b^5}$ is the dimensionless discharge in the fishway model, Y_o/b is the relative flow depth, and α, λ are coefficients relating the dimensionless discharge and the relative flow depth. It has been verified that the values obtained for all the different cases tested matched a linear relationship, that is to say, in every case where $\lambda=1$, and that the α coefficient depended on the configuration of baffles and the slope. The trivial condition is $Y_o=0$ when Q=0 has been imposed on the regression straight line, which implies that the independent term does not exist.

The experimental results: relative depth Y_o/b versus the nondimensional discharge are given in Fig. 4a, and the corresponding flow equations are shown in Table 3. The α values are proportional to the slope. A higher value for the proportionality factor (steepest line) means that for the same discharge the depth reached is lower and therefore the velocity profiles should increase, which implies a greater efficiency in conveyance.

The designs were also compared by grouping the experimental results obtained for both slopes; for this reason S_o was included in the nondimensional discharge Q^* (Equation 1). The values in the fishway model and in the equations are presented the Fig. 4b and the Table 3, respectively. Although the performance of both designs was very similar for each slope, it was also observed that given the same depth value in both designs, it was the T1 configuration that had the lower discharges.

A comparison between our results and the ones obtained by Rajaratnam *et al.* (1992) was carried out including designs 6, 16 and 18 (Fig 1). The discharge was non-dimensionalized by Q* [Eq.1] and the results were converted to an standard prototype values (Clay, C.H. 1995) with 0.305 m wide slot (b=0.305 m) using Froudian scaling formulae. The characteristic length b_o, was redefined in the results by Rajaratnam (1992), using the real slot length, b. The experimental observations converted to the standard prototype are shown in Fig. 5. The discharge-depth equations were found with the condition of $Y_o=0$ when Q=0 (Table 4) which also includes the values provided by Wu *et al.* (1999) for the D18 design. The results obtained show

that for designs D16 and T1, which are very similar in construction, the discharges equations are also very similar, while for T2 design (similar to D6 in construction) the value of its proportional constant is notably larger. The simplicity of T2 design versus T1 design provides a greater conveyance capacity which explains the higher values in the proportionality coefficient. The lower value of the discharge coefficient in D6 design versus D16 design does not appear to have a physical explanation.

DEPTH DISTRIBUITON

The average depth at the middle transverse section has been chosen to verify the performance of the design, but it is also important to know the values of other characteristic depths as Y_{max}, Y_b, Y_m and Y_{min}. Each of these provides us with information on a particular feature of the fishway: wall design criteria (Y_{max}), the limitations that depth may impose on the passage of fish (Y_{min}) as well as giving the depth at critical sections (Y_b).

A linear relationship has been found between each of the different characteristic depths and the relative flow depth at the middle transverse section Y_o/b,

$$Y/b = \alpha' \left(Y_0/b\right) + \beta' \qquad [5]$$

where Y stands for any of the characteristic depths, α',β' are coefficients which depend on the related characteristic depths, as well as on the slope and on the configuration of the baffles. These relationships can be found in Table 3. The depth at the slot was found to have a value that was quite similar to the average depth in the pool.

In Fig. 6, the experimental results for the different characteristic depths versus Y_o/b are shown, along with the corresponding equations (straight lines graphs) for T2 design for a slope 5,7%. It is suggested that the experimental relations between the different depths should not be extrapolated for very low depth values, since, for the near zero discharge values, all depth values will converge at a null value. Additional effects such as surface tension forces will come into play when discharges are so small.

WATER SURFACE

Typical level contours can be observed in Fig. 7, in the four experimental situations studied and with a single discharge of 0.065 m^3/s. There is always a region of great depths just upstream of the slot as well as in the region downstream of the pool, nearest to the larger baffles. At the slot point itself there is a sharp drop in the depth and continuing along down the slot, in the direction of the jet, there is a region of minimum depths as a consequence of such decay. Depth patterns are quite independent of flow rates.

Since the configurations patterns of the water surface are independent of discharges, the performance of the vertical slot fishway remains stable with variations in flow rates. This stability is one of the most important characteristic in terms of the application of vertical slot fishway.

In spite of similar performance of the two configurations, we must remember that the shallowest region is located in the T1 design near the longitudinal central line. This is due to the different orientation of the main flow when it comes out of the slot, approximately parallel to the sidewalls in the T2 configurations and moving diagonal up to the far corner in the T1 configuration. Another noticeable difference is seen in the different configurations of the level lines joining these water surface points with the same depth, which in design T2 are perpendicular to the longitudinal axis (Fig 7c, profile AA´) while in design T1 they are perpendicular to diagonal line (Fig. 7a, profile BB´).

Water depths measured in the section parallel to the longitudinal axis, joining both slots (AA´) and with a discharge of 0.065 m^3/s, are shown in Fig. 8. In both designs the largest depth values were reached for the slope of S_o=10,054%. There is a rapid drop of depth which corresponds to the transition from the slot to the depression region immediately below, and a gradual increase untill the next slot is reached. The greatest relative drop in the depression pertained to a slope of 10,054%.

VELOCITY FIELD AND FLOW PATTERNS

The configurations of the velocity fields in the pools are one of the main factors used to determine the characteristics of the flow. Velocity fields taken in planes parallel to the bed are shown in Fig. 9, where horizontal components (V_x and V_y) of the velocity vectors can be seen. A reference vector is included in order to make the comprehension of the figures more intuitive.

Generally, two different kinds of regions are formed: one, which will be referred to as the direct flow region, where the flow circulates in a curved trajectory at a high speed from one slot to the next downstream; and the others, which will be refered to as recirculation regions, characterized by slower velocities, flow in the opposite direction, owing to the existence of vertical axis eddies. Two recirculation regions of different sizes and separated by the direct flow region, are shown in the flow patterns; the larger one is located close to the long baffles and the smaller one, near the short baffles.

In design T1 the streamtrace of the main flow travels towards the center of the pool continuing up until it reaches the slot downstream in a curved trajectory, whereas in design T2 the streamtrace of the main flow travels in a straighter direction, parallel to the flume sidewalls from one slot to the next, creating, as a consequence, a minor mixing of the jet coming from the slot and the water volume in the pool. This difference in the configurations of the main flow trajectory is one of the main reasons why it is necessary to explain the different hydraulic performance of both designs.

The recirculation regions for T1 design vary in shape according to the flow rates and the slope of the model. In design T1 for S_o=5,7%, two eddy areas are formed, the larger one located between the long baffles and the smaller one located between the short baffles (Fig. 10a). As the flow rate increased the larger eddy area moves somewhat farther upstream, while samaller one increases slightly in size. For S_o=10,054% the flow presents two different patterns. The pattern for Q^A<2.75 is similar to the one that was established for slope of 5,7%. When Q^A>2.75, the flow pattern shows two differentiated eddies which can be clearly seen in the recirculation regions between the long baffles (Fig. 9a and 9b, sketched in Fig. 10a and Fig. 10b).

A circulation pattern was found for T2 design (Fig. 9c, 9d, and 10c) for any discharge or slope considered. The recirculation region located between the long baffles occupies almost the whole of the pool, offering a very large-resting zone to upstream moving fish. The eddy near the short baffles is much smaller in size than the one in T1 design, and shows a slight increase in size with increasing slope

In general the T1 configuration has a hydraulic performance involving low velocities, which is believed to be a positive contribution in practical applications. The T2 design offers flow patterns in which recirculation and direct flow regions are more clearly differentiated, as well as larger resting zones.

The velocity fields were also studied in vertical planes parallel to the longitudinal axis of the fishway (plane XZ) to understand the evolution of the velocity at different water levels. The V_x-V_z velocity components can be observed in Fig. 11 in a vertical plane parallel to the longitudinal axis of the fishway. Both sections represented belong to the direct flow region in a straight line from slot to slot. It is interesting to note that the development of the velocity patterns is independent of the distance from the bed; similarly, it is possible to detect the minor importance of the vertical component of the velocity. This bidimensionality of the flow can be seen more clearly inside the direct flow region where the V_z component is very close to its null value.

The study of the horizontal velocity fields for a given discharge in different planes parallel to the channel wall points to the existence of similar velocities all along the water column. The evolution of the component V_x all along the water column in the T2 design and for S_o=10.055%, can be seen in Fig. 12a and in Fig. 12b for T1 design and S_o=5,7%. The velocity value proves to be almost independent of the location within the water column for both slopes and both designs.

The bidimensionality of the flow establishes the main difference between the water flow in vertical slot fishways and flow in other fishway types (pool and weir type and Denil type) in which the flow is three-dimensional. Since there are no variations in the vertical direction of the velocity fields, fish may choose any swimming depth according to their preferences.

VELOCITY-DISCHARGE RELATIONSHIPS

A knowledge of the velocity patterns and the velocity distribution along the water column clearly indicates the need to study the dependence of the velocity values on the discharges in the fishway. In Fig. 13 the value of the depth average velocity versus the discharge was represented at several points for two experimental situations.

It is interesting to note that the velocity at any point along the pool depends on the position of the point itself, on the configurations of the design and on the fishway slope; but it is not related to the discharge. This agrees with the linear relationship found between depth and discharge. The independence of the velocity versus the discharge proves the stability in the performance of these kind of fishways, without regulation arrangements on the discharge inlet.

The most critical section in the fishway for the passage of the fish is the slot, since it is an unavoidable route and also because the highest velocities are reached in the area surrounding it. For this reason a specific analysis of the slot velocity was carried out in relation to the discharge and distance to the bed. In Fig. 14 the evolution of the slot velocity can be seen versus the distance of measurement planes from the bed for several discharges. The uniformity of the velocity can be observed all along the water column. Similar results have been obtained for the rest of the experimental situations.

Figure 15 shows a relationship between the depth averaged velocity at slot (V_{mb}) and the discharge. It is clear that not only does the velocity at the slot remain the same throughout the water column (Fig. 14) but for a given fishway slope, it also proves to be independent of the discharge (Fig. 15). The values of discharge-averaged velocity of depth average velocity at a slot are shown in Table 5. It has been verified that the velocity at the slot depends, apart from the slot width, on the fishway slope which (increases with it) and on the baffles configuration (T2 model obtains the highest velocities).

ENERGY DISSIPATION

The efficiency of the vertical slot fishway as a passage for migratory fish depends, among other factors, on the turbulence and the aeration in the pools. A simple indicator of these parameters is the energy dissipation inside the pools per unit volume. The higher the energy dissipation value, the more difficult it becomes for fish to travel upstream. According to the formulation used in the pool and weir fishways (Larinier *et al.* 1998), the energy dissipation inside the pool per unit volume is defined as:

$$E = \frac{\rho g Q \Delta h}{L W Y_0} = \frac{\rho g Q S_o}{W Y_0} \qquad [6]$$

where ρ=mass density of water, L and W are length and width of the pool respectively.

The experimental results in Fig. 16 show that energy dissipation remains independent of discharge and that both configurations show very similar values.

If, taking into account equation 6, the relationship $Q^A = \alpha\left(\frac{Y_0}{b}\right)$ found for each of the four experimental situations assayed (shown in Table 3), and the definition of S_0 as $S_0 = \Delta h/L$, the following may be obtained:

$$E = \rho\alpha S_o (gb)^{3/2} / W \qquad [7]$$

which clarly demonstrates that the value of the energy dissipated depends exclusively on the slope (α, S_o) and on the baffles configuration (α, b, W) and is independent of flow rate. In Table 6 the energy dissipated in the 5,7% slope is very similar in both configurations, with very little difference observed. For the larger of the slopes (S_o=10.054%) the difference is slightly greater, and is higher in the T2 design, which should mean that the objective of the passage of the fish is less efficient.

The experimental results of the fishway model has been converted, using Froudian scaling formulae, to the full scale (standard prototype with a slot width b=0.305 m). The mean energy dissipation values of the overall discharges are shown in Table 6.

The maximum values recommended by Larinier et al, 1998 for the energy dissipation are 150 W/m^3 and 200 W/m^3 depending on the species and size of fish, although in small fishways, they can increase up to 400 W/m^3. As a consequence of these maximum values of the energy dissipation, which must be interpreted wisely, both designs could be successfuly employed for S_o=5,7% with even larger slot widths (than that commonly used b=0.305 m). On the other hand, a slope of 10,054% is slightly more selective in terms of fish passage.

It must be highlighted that this data analisis presents a rough approach to the energy dissipation patterns in the pool, and further research is needed.

KINETIC TURBULENT ENERGY

The estimation of turbulence parameters (turbulent kinetic energy, k, dissipation rates, ε, Reynolds stress) based on the velocity measurements in vertical slot fishways is of special interest given that high levels of turbulence may disorient the fish, and also because there is very little information on this subject in the bibliography.

This article presents the turbulent kinetic energy since the low sampling frequency (15 Hz) and the probe size (0.08 cm^3) would not allow us to calculate other variables, such as ε. Owing to the small magnitude of the Doppler noise scale, it was not able to be considered in the calculation of the turbulent kinetic energy. Therefore, the velocity time series, $V_i(t)$ was

divided into a time average and a turbulent component. The turbulent component, v_i' is the root-mean-square of the turbulent velocity fluctuations and it is equal to the standard deviation of the time series.

$$V_i(t) = V_i + v_i' \qquad [8]$$

These velocity data were used to generate calculations of the turbulent kinetic energy (k) as defined by (Rodi, W., 1980):

$$k = \frac{1}{2}\left(v_x'^2 + v_y'^2 + v_z'^2\right) \qquad [9]$$

By using a preliminary approach, we have attempted to quantify the turbulent kinetic energy and to understand its distribution in the two designs of vertical slot fishways. For this purpose, we have first presented a comparative table (Table 7) of the specific values of the turbulent kinetic energy, k. Each value measured at a given point in the pool is defined by five factors: type of design, slope, flow depth, distance from the bed (h), and position in the pool (Z_{low}, Z_{inter}, Z_{high}) depending on whether the point belongs to an area of low, intermediate or high turbulence (as defined in Fig.17). On the basis of a more in-depth analysis, these points were selected as being representative of areas with greater turbulence, zones providing the best conditions for the fish to rest and the direct flow region.

Fig. 17 shows the typical distributions of the contour lines of turbulent kinetic energy on planes which are parallel to the bed in both experimental situations. Also exhibited is the mean averaged water velocity over time at the vector, Vx-Vy. The maximum k value is found in the areas near the slots and it is high in the direct flow zones defined in the flow circulation patterns (Fig. 10). In the recirculation areas k reaches its lowest values.

The dependency of the turbulent kinetic energy on depth was examined. As shown in Fig. 18 where k-Q was drawn for a T1 design with a slope of S_o=10.054%, in both Z_{low} and Z_{inter} k is unaffected by changes in depth. For Z_{high} there was a wide range of experimental results that did not show any clear trends. In the other experimental situations, there was a repetition of the scheme outlined above.

In general, in areas of low and intermediate intensity, the turbulent kinetic energy is independent of the vertical distance from the bed. However, in the high turbulence zone, Z_{high}, a greater turbulence value was found near the surface and the bed, as demonstrated in Fig. 19 where k is compared to h. In this figure the turbulent kinetic energy was made dimensionless using the discharge-averaged mean velocity at slot, V_{mb}^{Q} (Table 5) for the zone with the highest intensity (Z_{high}) where the greatest magnitude in the range of experimental measurements was found.

$$k_A = k\left(b \Big/ V_{mb}^{Q} \sqrt{LW} \right)^2 \qquad [10]$$

Intermediate depths and a logarithmic scale are given to make it easier to clearly appreciate the appropriate grouping of the data based on the model design.

CONCLUSIONS.

Considering the usual slopes, the performance of two particular vertical slot fishway designs has been studied using a wide range of discharges. A linear relationship was found between the dimensionless discharge and the average depth at the middle transverse section, as well as some linear trends among the different characteristic water depths. Hydraulic behaviour patterns were observed in both types. Two clearly defined regions were able to be distinguished in these patterns: the recirculation regions characterized by low velocities, horizontal eddies and reversed flows; and the direct flow region characterized by bidimensionality and maximum velocities.

Velocity fields were measured the water volume in the pool, showing that in general the vertical component of the velocity is close to its null value. The uniformity of the velocity value was verified all along the vertical water column. It was concluded that, for a given slope of each fishway configuration, the velocity in the pool is independent of discharge at every point, including the slot. Acceptable values of the energy dissipation inside the pool were found to be an indicator of the ability of fish to pass through.

ACKNOWLEDGMENTS

The authors would like to thank the CITEEC staff (Centro de Innovación Tecnolóxica en Edificación e Enxeñería Civil) at the Universidade de A Coruña (Spain), without whose help the development of experimental work essential to this research would not have been possible, as well as the Spanish Ministry of Science and Technology, which funded this research project (CICYT-HID-1999-0297).

APENDIX I. REFERENCES

Beach, M.H. (1984). "Fish pass design. Criteria of the design and approval of fish passes and other structures to facilitate the passage of migratory fishes in rivers". *Fish. Res. Tech. Rep*. 78. MAFF Direct. Fish. Res., Lowestoft.

Clay, C.H. (1995). *Design of fishways and other fish facilities*. Lewis Publisher, Boca Raton.

Kamula, R. (2001). "Flow over weirs with application to fish passage facilities". Academic Disertation. Departament of Process and Environmental Engineering, University of Oulu, Oulu. Finland.

Kraus, N.C., Lohrmann, A., and Cabrera, R. (1994). "New acoustic meter for measuring 3D laboratory flows.". *J. Hydr. Engrg*, ASCE, Vol. 120, No. 3, 406-412.

Larinier, M., Porcher, J.P., Travede, F., Gosset, C. (1998). *Passes à poissons. Expertise conception des ouvrages de franchissement*. Conseil Supérieur De La Pêche, Paris. France.

Nikora, V.I. and Goring, D.G. (1998). "ADV measurements of turbulence: can we improve their interpretation?". *J. Hydr. Engrg*, ASCE, Vol. 124, No. 6, 630-634.

Rajaratnam, N., Katopodis, C., and Solanki, S. (1992). "New designs for vertical slot fishways". *Can. J. Civ. Engrg.*, Ottawa, Canada, 19(3). 402-414.

Rajaratnam, N., Van der Vinne, G., and Katopodis, C. (1986). "Hydraulics of vertical slot fishways". *J. Hydr. Engrg*, ASCE, Vol. 112, No. 10, 909-927.

Rodi, W. (1980). *Turbulence models and their application in hydraulics*. IAHR Monograph. Delft, The Netherlands.

Teijeiro, T. (2001). "Criterios de diseño de escalas de peces de hendidura vertical", Ph. D. Thesis. Departamento de Enxeñería Agroforestal, Universidade de Santiago de Compostela, Lugo. Spain.

Wu, S., Rajaratnam, N. and Katopodis, C. (1999). "Structure of flow in vertical slot fishway". *J. Hydr. Engrg*, ASCE, Vol. 125, No. 4, 351-359.

APENDIX II. NOTATION

The following symbols are used in this paper:

b = slot real width;

b_o = slot characteristic width from Rajaratnam *et al*. 1992;

C_d = coefficient of discharge;

E = energy dissipation;

g = acceleration due to gravity;

h = vertical distance from the bed;

k, k_A = turbulent kinetic energy and dimensionless turbulent kinetic energy;

L = length of pool;

Q = discharge;

Q^* = dimensionless discharge from Rajaratnam *et al.* (1992,1986);

Q^{**} = dimensionless discharge from Kamula, R. (2001);

Q^A = dimensionless discharge from present data;

S_0 = bed slope;

V_m = depth-average velocity;

V_b = velocity at slot;

V_{mb} = depth-average velocity at slot;

V_{mb}^{Q} = discharge and depth-averge velocity at slot;

V_x ,V_y,V_z = velocity at a point on X,Y,Z axis;

Y = depth of flow (measured in vertical) ;

Y_o = uniform flow depth, mean depth at middle traverse section (measured in vertical);

Y_b = flow depth at slot (measured in vertical);

Y_m = mean flow depth at pool (measured in vertical);

Y_{max} = maximum flow depth at pool (measured in vertical);

Y_{min} = minimum flow depth at pool (measured in vertical);

W = width of pool;

Δh = difference between upstream and downstream depth at slot;

ρ = density of fluid;

Table 1. Summary of present experiments.

	Depth				Velocity			
Design	T1		T2		T1		T2	
S_o	5,7%	10,054%	5,7%	10,054%	5,7%	10,054%	5,7%	10,054%
Range Q	16-85	35-115	25-85	35-125	16-85	35-125	25-185	35-125
Nº Discharge	8	9	7	9	8	9	7	9
Points/Level	89	111	109	109	101	140	132	132

Table 2. Summary of experimental results. All measurements are model data with b=0.16 m in the T1 design and b=0.15 m in the T2 design.

Des.	S_o	Q (m^3/s)	Q^A	Y_o (m)	Y_b (m)	Y_m (m)	Y_{max} (m)	Y_{min} (m)	V_b (m/s)	C_d	E_d (W/m^3)
T1	5,7	0.0159	0.4945	0.125	0.158	0.130	0.175	0.107	0.86	0.73	71.81
T1	5,7	0.0209	0.6529	0.176	0.195	0.179	0.215	0.143	0.85	0.79	67.13
T1	5,7	0.0246	0.7669	0.190	0.230	0.197	0.236	0.167	0.79	0.85	72.99
T1	5,7	0.0341	1.0624	0.253	0.306	0.262	0.313	0.212	0.88	0.80	75.94
T1	5,7	0.0458	1.4277	0.379	0.406	0.386	0.425	0.356	0.84	0.83	68.25
T1	5,7	0.0540	1.6827	0.437	0.476	0.445	0.483	0.400	0.87	0.82	69.74
T1	5,7	0.0641	1.9983	0.488	0.529	0.495	0.540	0.453	0.89	0.85	74.18
T1	5,7	0.0741	2.3104	0.604	0.604	0.608	0.652	0.562	0.88	0.87	69.35
T1	5,7	0.0859	2.6791	0.665	0.697	0.674	0.711	0.628	0.85	0.91	72.97
T1	10.05	0.0348	1.0847	0.155	0.201	0.171	0.253	0.093	1.25	0.86	223.25
T1	10.05	0.0445	1.3879	0.247	0.278	0.262	0.357	0.178	1.20	0.83	179.76
T1	10.05	0.0551	1.7174	0.314	0.371	0.331	0.420	0.242	1.21	0.77	174.88
T1	10.05	0.0643	2.0059	0.366	0.406	0.378	0.469	0.288	1.19	0.83	175.00
T1	10.05	0.0751	2.3425	0.436	0.505	0.452	0.541	0.363	1.25	0.75	171.72
T1	10.05	0.0849	2.6482	0.489	0.553	0.507	0.597	0.429	1.00	0.96	172.94
T1	10.05	0.0945	2.9478	0.526	0.561	0.541	0.634	0.443	1.17	0.90	179.16
T1	10.05	0.1044	3.2554	0.581	0.621	0.596	0.690	0.513	1.05	1.01	179.11
T1	10.05	0.1150	3.5856	0.641	0.681	0.656	0.755	0.556	1.06	1.00	178.79
T2	5,7	0.0160	0.5855	0.102	0.109	0.152	0.061	0.682	0.95	1.05	88.18
T2	5,7	0.0250	0.9153	0.169	0.180	0.225	0.122	1.125	0.93	0.97	83.64
T2	5,7	0.0350	1.2811	0.263	0.274	0.323	0.214	1.750	0.99	0.84	75.23
T2	5,7	0.0453	1.6585	0.350	0.362	0.408	0.298	2.336	1.00	0.81	72.96
T2	5,7	0.0540	1.9772	0.439	0.449	0.497	0.376	2.928	0.97	0.82	69.39
T2	5,7	0.0639	2.3405	0.524	0.531	0.577	0.475	3.495	1.09	0.72	68.82
T2	5,7	0.0741	2.7131	0.606	0.613	0.660	0.552	4.040	0.87	0.92	69.02
T2	5,7	0.0840	3.0785	0.670	0.679	0.732	0.615	4.468	0.96	0.82	70.81
T2	10.05	0.0253	0.9277	0.134	0.138	0.208	0.080	0.892	1.14	0.75	188.43
T2	10.05	0.0352	1.2912	0.206	0.202	0.276	0.132	1.375	1.23	0.79	170.20
T2	10.05	0.0453	1.6601	0.248	0.251	0.329	0.152	1.656	1.32	0.79	181.73
T2	10.05	0.0549	2.0100	0.307	0.311	0.405	0.212	2.048	1.32	0.80	177.95
T2	10.05	0.0645	2.3644	0.371	0.372	0.461	0.275	2.471	1.27	0.85	173.48
T2	10.05	0.0746	2.7325	0.431	0.432	0.515	0.330	2.873	1.31	0.83	172.42
T2	10.05	0.0838	3.0718	0.483	0.480	0.569	0.380	3.222	1.33	0.83	172.81
T2	10.05	0.0954	3.4955	0.536	0.539	0.623	0.437	3.577	1.30	0.85	177.17
T2	10.05	0.1048	3.8398	0.578	0.578	0.657	0.483	3.853	1.30	0.87	180.66
T2	10.05	0.1151	4.2177	0.615	0.612	0.714	0.505	4.100	1.46	0.80	186.50
T2	10.05	0.1248	4.5739	0.650	0.649	0.745	0.536	4.332	1.28	0.91	191.39

Table 3. Flow equations, relationship between dimensionless discharge and relative depths. In parentheses, correlation coefficent (r^2).

Design	So	Q^A	Y_{min}/b	Y_b/b	Y_{max}/b	Y_m/b	Q*
T1	5,7%	0.631Yo/b (0.9946)	0.9739Yo/b-0.1409 (0.9986)	0.9758Yo/b+0.2512 (0.9944)	0.9993Yo/b+0.3018 (0.9992)	1.015Yo/b (0.9998)	2.7289Yo/b (0.9872)
	10.054%	0.8888Yo/b (0.9889)	0.9742Yo/b - 0.3822 (0.9979)	1.0008Yo/b+0.2918 (0.9933)	1.021Yo/b+0.6133 (0.9996)	1.033Yo/b (0.9987)	
T2	5,7%	0.6867Yo/b (0.9903)	0.9789Yo/b-0.2871 (0.9994)	1.031Yo/b+0.0407 (0.9983)	1.0065Yo/b+0.3583 (0.9997)	1.0183Yo/b (0.9994)	3.0382Yo/b (0.9783)
	10,054%	0.9988Yo/b (0.9903)	0.9196Yo/b-0.4069 (0.9965)	0.9949Yo/b+0.2826 (0.9949)	1.0323Yo/b+0.4811 (0.9982)	1.0002Yo/b (0.9997)	

Table 4. Relationship between dimensionless discharge and relative depth with $Q^* = Q/\sqrt{gS_o b_o^5}$. In parentheses, correlation coefficent (r^2).

Present Data	Rajaratnam *et al.* (1992)		Wu *et al.* (1999)
$Q^*_{T1} = 2.7289\, Y_o/b$ (0.9872)	$Q^*_{D16} = 2.6878\, Y_o/b$ (0.9981)	$Q^*_{D18} = 3.7745\, Y_o/b$ (0.9761)	$Q^*_{D18} = 3.75\, Y_o/b$
$Q^*_{T2} = 3.30382\, Y_o/b$ (0.9783)	$Q^*_{D6} = 2.2787\, Y_o/b$ (0.9406)		

Table 5. Discharge-averaged mean velocity at slot.

V_{mb}^{Q} (cm/s)		
Design	So=5,7%	So=10.054%
T1	85.63	115.21
T2	96.99	126.47

Table 6. Energy dissipation rate for fishway model and for standard prototype with a slot width b=0.305 m.

E (W/m³)		
Model		
Design	So=5,7%	So=10.054%
T1	71.44	177.49
T2	70.57	181.06
Prototype (b=0.305 m)		
Design	So=5,7%	So=10.054%
T1	98.63	245.05
T2	100.63	258.18

Table 7. Specific values of turbulent kinetic energy.

		k (cm^2/s^2)								
		Q=65 l/s			Q=75 l/s			Q=85 l/s		
Type, S_o	h	Z_{low}	Z_{inter}	Z_{high}	Z_{low}	Z_{inter}	Z_{high}	Z_{low}	Z_{inter}	Z_{high}
	h_{bed}	148	529	1958	342	677	1797	122	722	1818
T1, 5%	$h_{25\ cm}$	168	810	863	194	889	1554	238	915	1281
	$h_{surface}$	331	927	1734	328	653	2211	249	565	3329
	h_{bed}	123	224	598	133	208	689	149	243	774
T2, 5%	$h_{25\ cm}$	142	498	355	103	222	378	160	219	464
	$h_{surface}$	216	371	1810	137	361	2955	184	580	1989
	h_{bed}	351	675	8890	298	797	3440	234	1000	3501
T1, 10%	$h_{15\ cm}$	232	1586	5450	363	1321	2035	382	1099	2822
	$h_{surface}$	171	1554	3404	181	1310	2983	285	998	3938
	h_{bed}	92	472	1080	167	384	1268	131	521	1643
T2, 10%	$h_{15\ cm}$	293	767	727	190	592	815	260	447	810
	$h_{surface}$	255	581	651	277	880	1389	287	1130	919

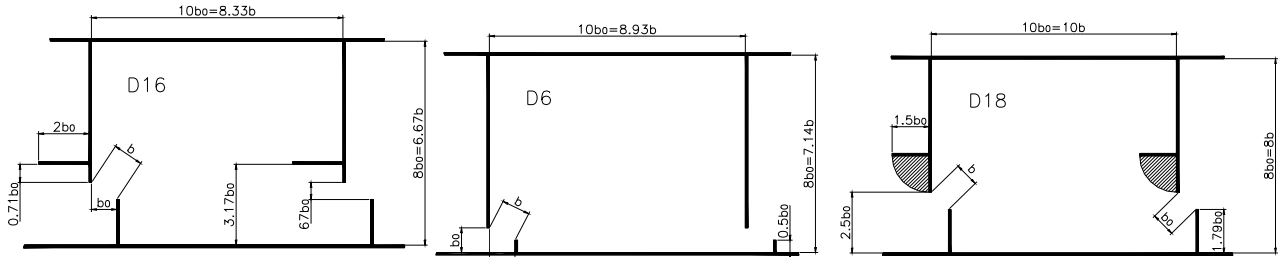

Fig. 1. Details of designs 6, 16 and 18, recommended for practical use by Rajaratnam *et al.* (1986, 1992).

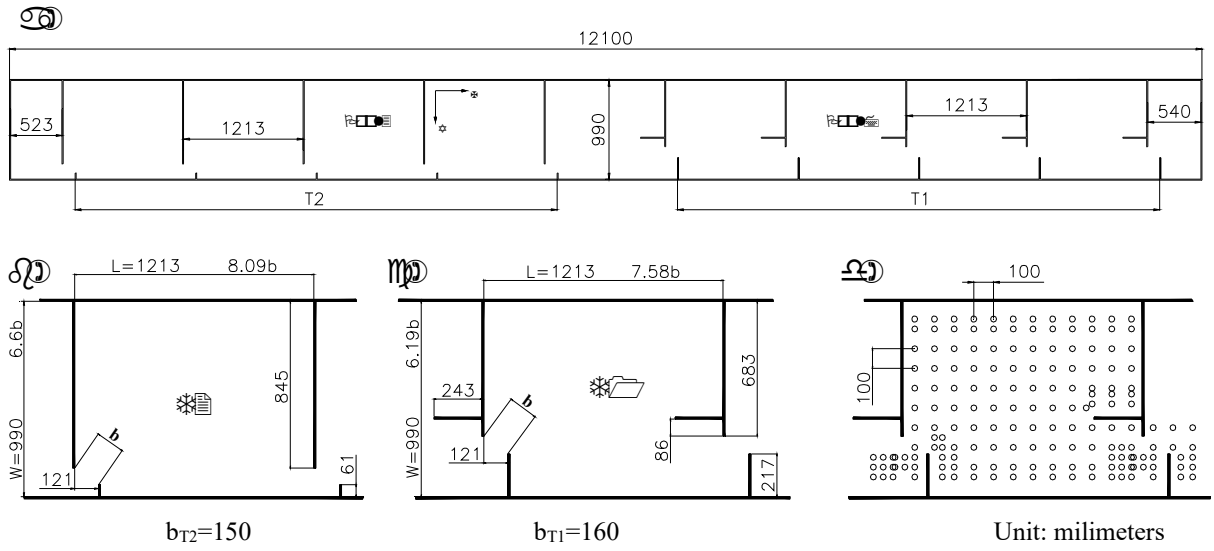

Fig. 2. a) Dimension of the laboratory model of a vertical slot fishway. b and c) Details of T1 and T2 designs. d) Data point mesh in a parallel plane to the bed for T1 design and a slope of 10,054%.

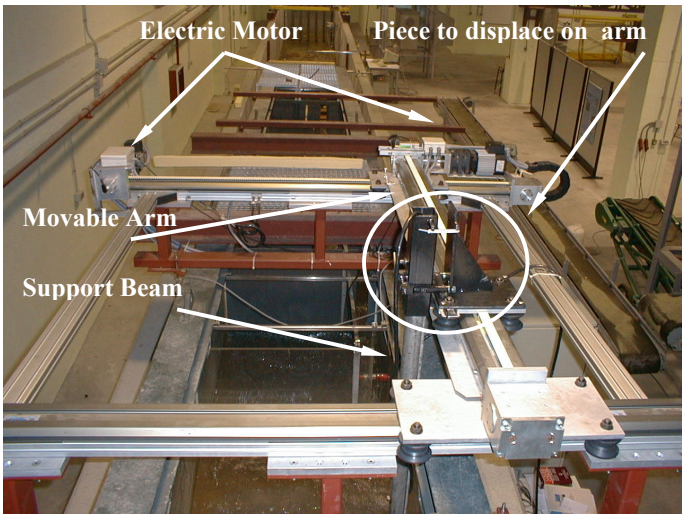

Fig. 3. Cartesian positioner used to place the measurement gauges automatically over the experimental pools.

a)

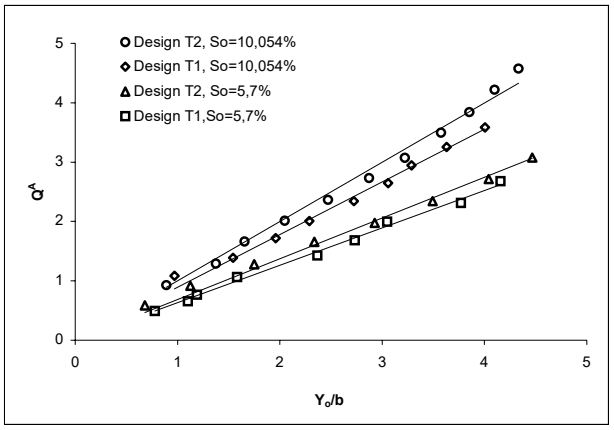

b)

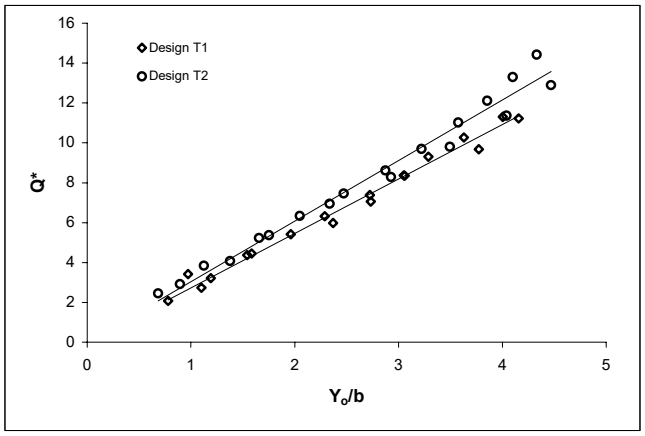

Fig. 4. Dimensionless relationship a) Q^A against Y_o/b, and b) Q^* against Y_o/b.

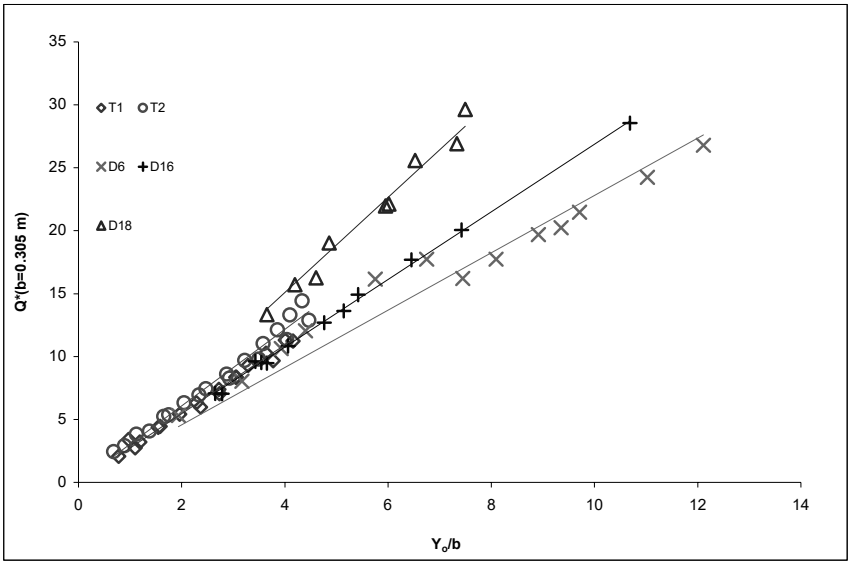

Fig. 5. Dimensionless relationship discharge against depth in a standard prototype (b=0.305 m) for several designs.

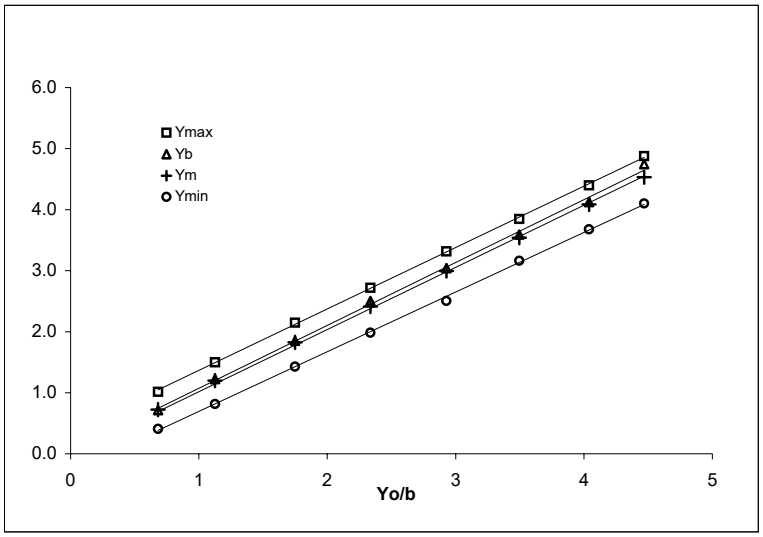

Fig. 6. Relationship between characteristic depths, in the T2 design for S_0=5,7%.

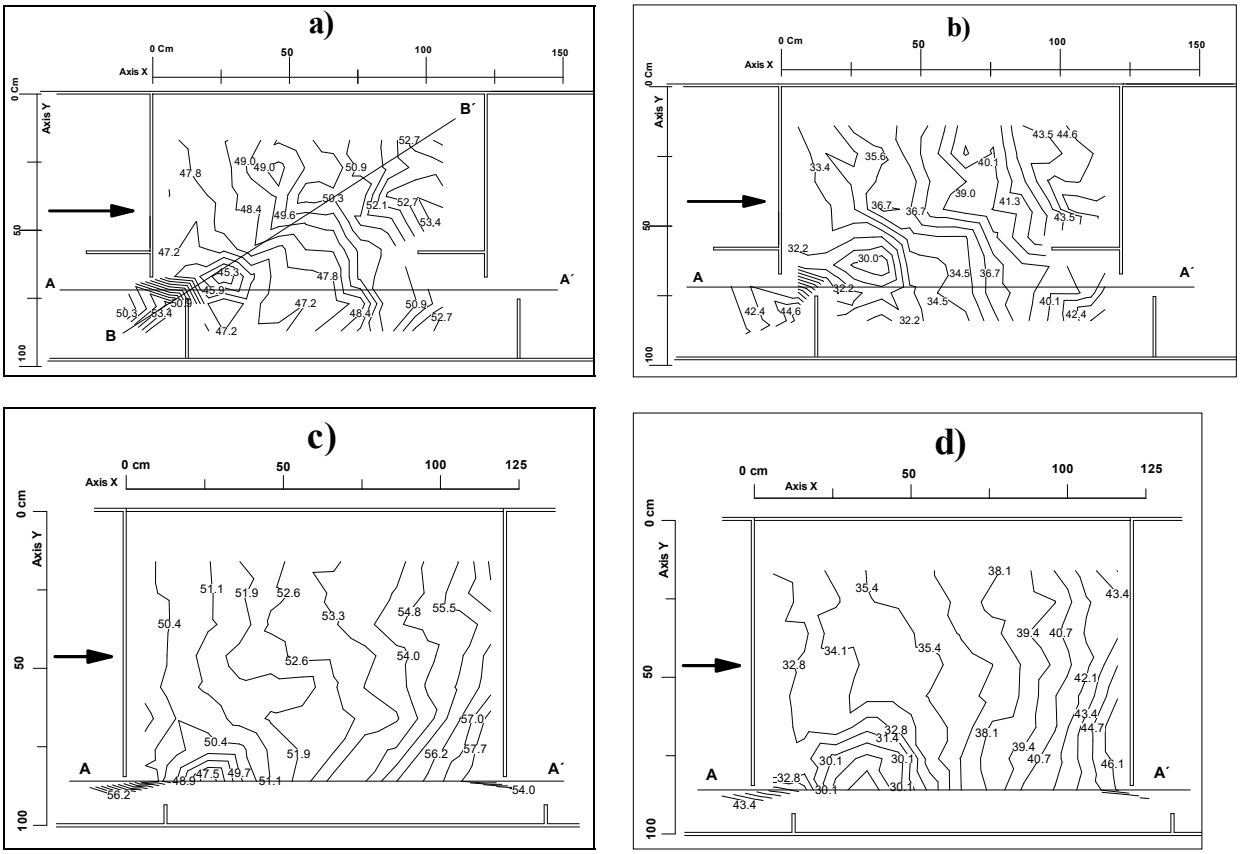

Fig. 7. Contour lines of water free surface in the fishway model, for a discharge Q=0.065 m^3. a) Design T1, S_o=5,7%. b) Design T1, S_o=10,054%. c) Design T2, S_o=5,7%. d) Design T2, S_o=10,054%.

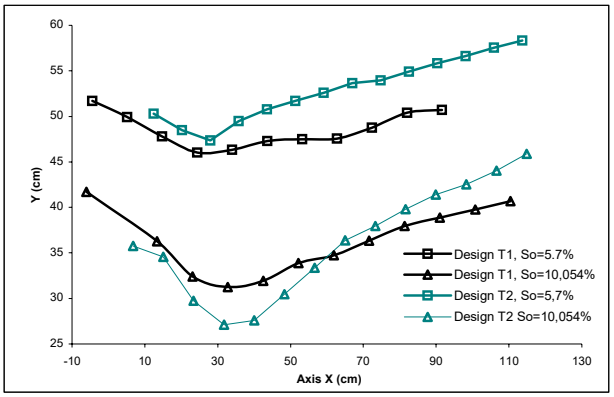

Fig. 8. Experimental depth values on a straight line linking two consecutive vertical slots, for discharge Q=0,065 m^3.

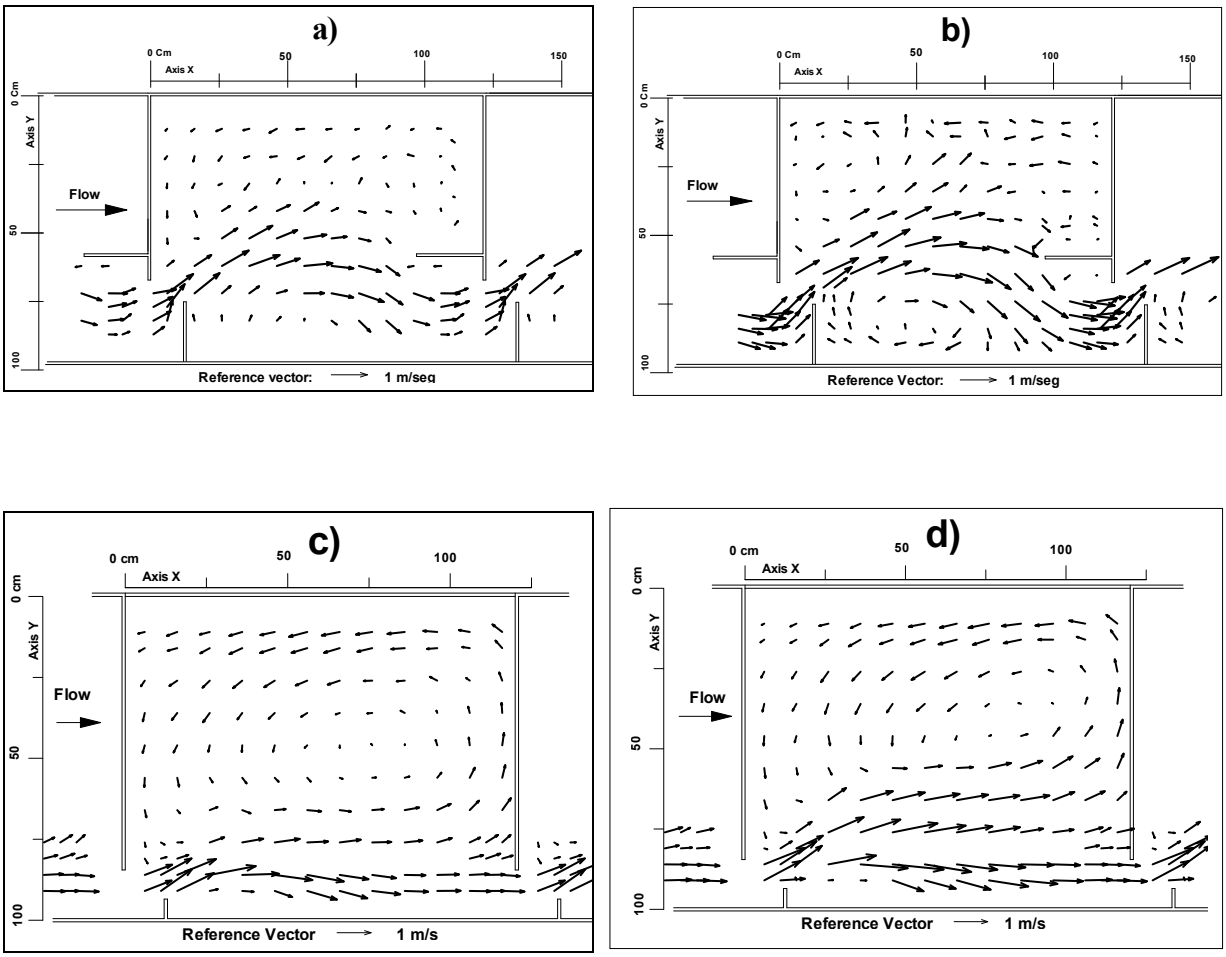

Fig. 9. Horizontal velocity fields, V_x-V_y in planes parallel to the bed for several experimental situations: a) Design T1, S=5,7%, Q=85 l/s, h=35 cm; b) Design T1, S=10,054%, Q=105 l/s, h=5 cm; c) Design T2, S=5,7%, Q=54 l/s, h=25 cm; d) Design T2, S=10,054%, Q=75 l/s, h=25 cm

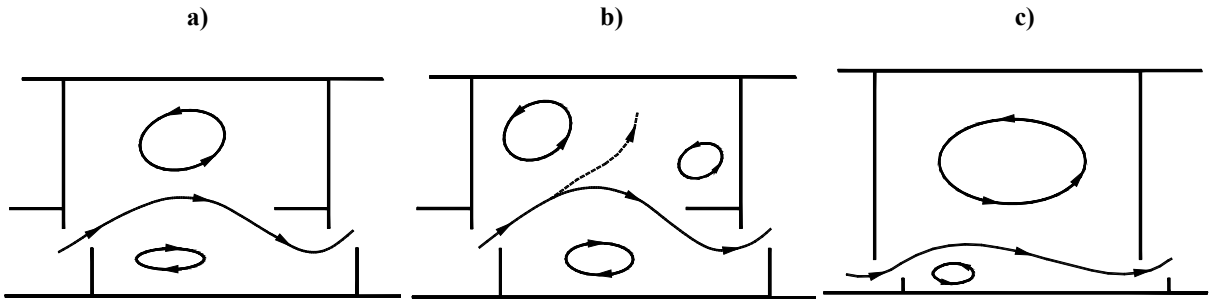

Fig. 10. Flow patterns in pools: a) Design T1, S_o=5,7%; and S_o=10.054% with Q^A<2.75. b) Design T1, S_o=10.054% with Q^A>2.75. c) Design T2.

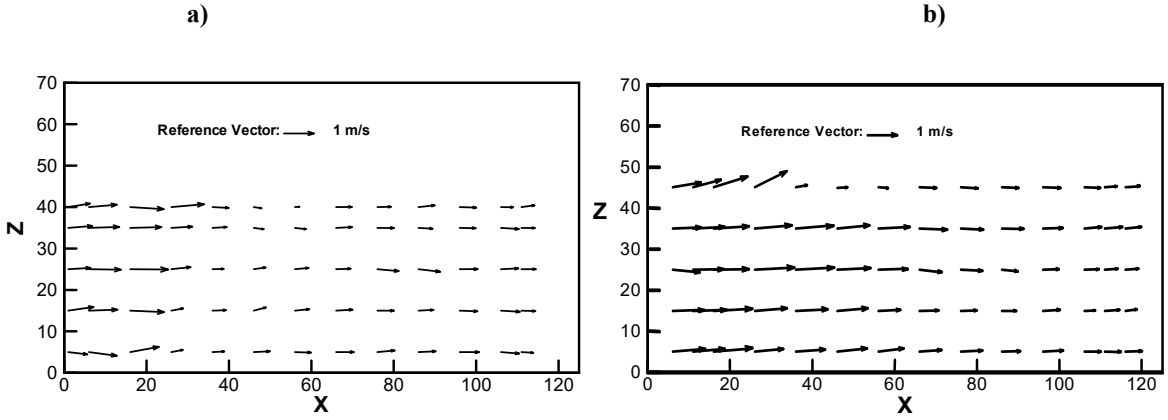

Unit: cm.

Fig. 11. Velocity fields, V_x-V_z in vertical planes parallel to longitudinal axis of fishway. a) T1 design, S_o=5,7%, Q=0,065 m^3, Y=72 cm b) T2 design, S_o=10,054%, Q=0,0746 m^3, Y=86 cm

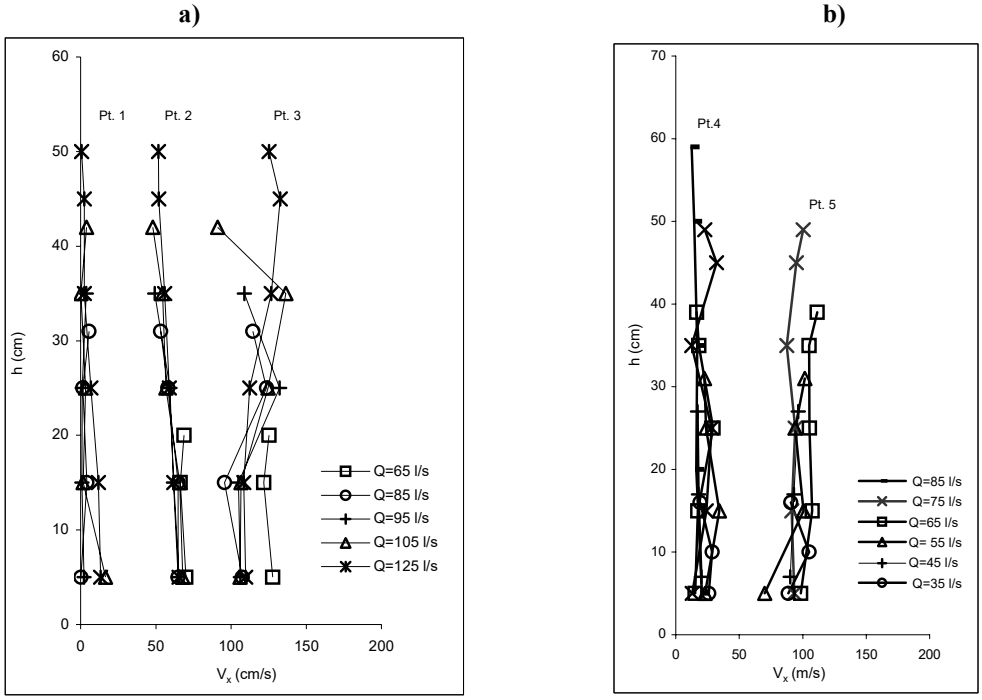

Fig. 12. Vertical distributions of velocity values at some points for several discharge. a) T2 design, S_0=10,054% in: Pt. 1 x=76 cm, y=46 cm; Pt. 2 x=76 cm, y=11 cm; and Pt. 3 x=56 cm, y=86 cm. b) T1 design, S_o=5.7% in: Pt. 4 x=36 cm, y=12 cm; and Pt. 5 x=36 cm, y=62 cm.

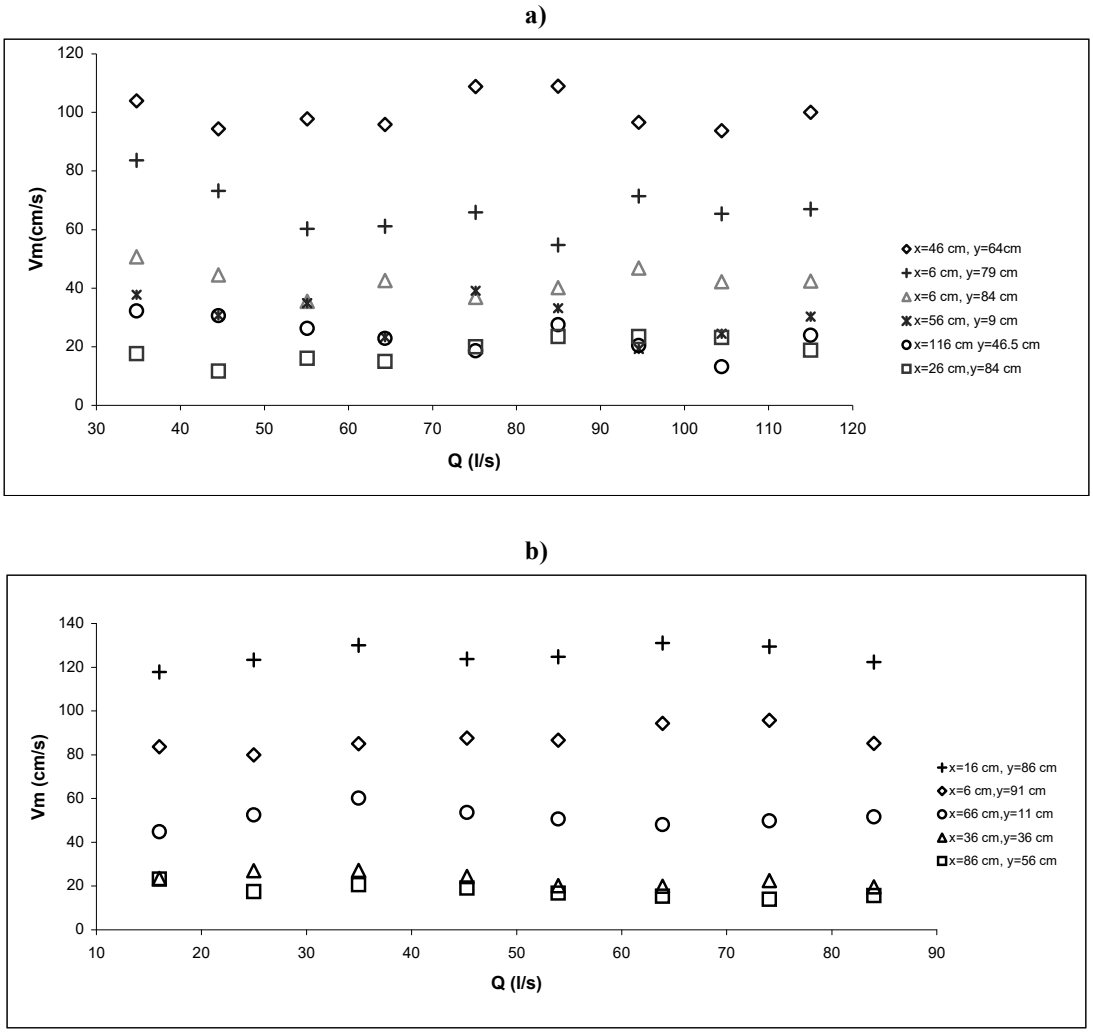

Fig. 13. Velocity evolution against discharge at several experiemental data points. a) T1 design, S_o=10.054; b) T2 design, S_o=5.-7%.

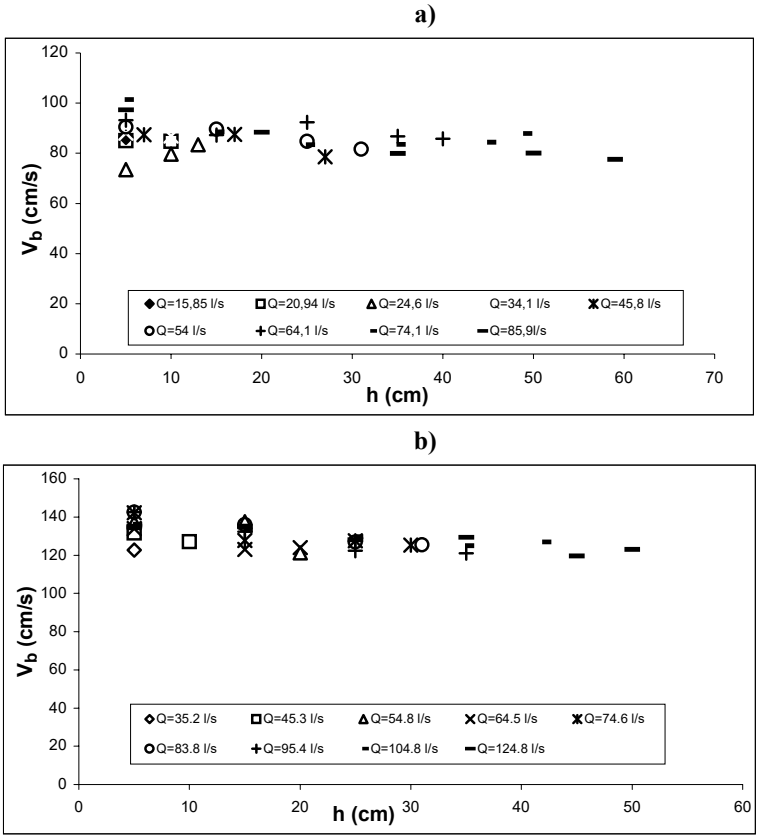

Fig. 14. Values of the slot velocity against distance to the bed for several discharges. a) T1 design, So=5.7%; b) T2 design, So=10.054%.

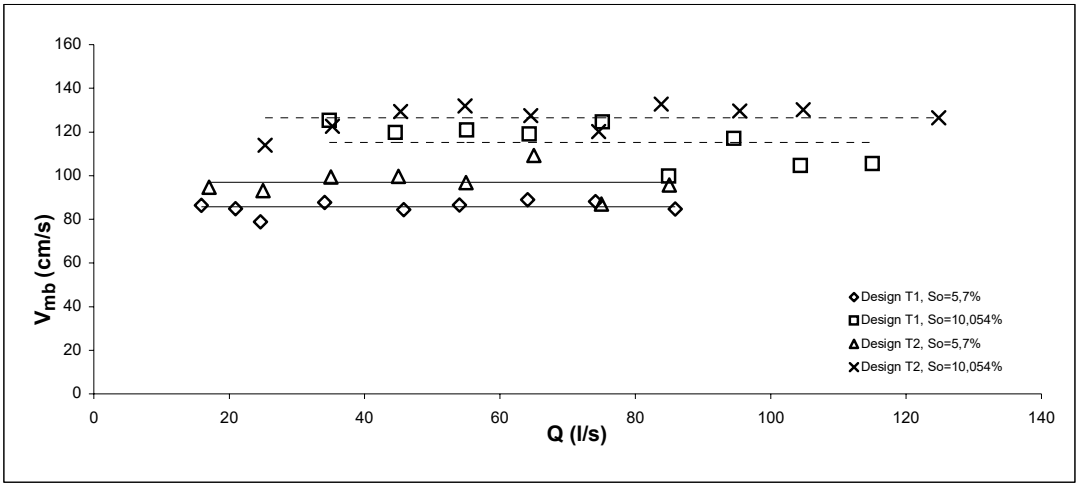

Fig. 15. Depth average slot velocities versus discharge.

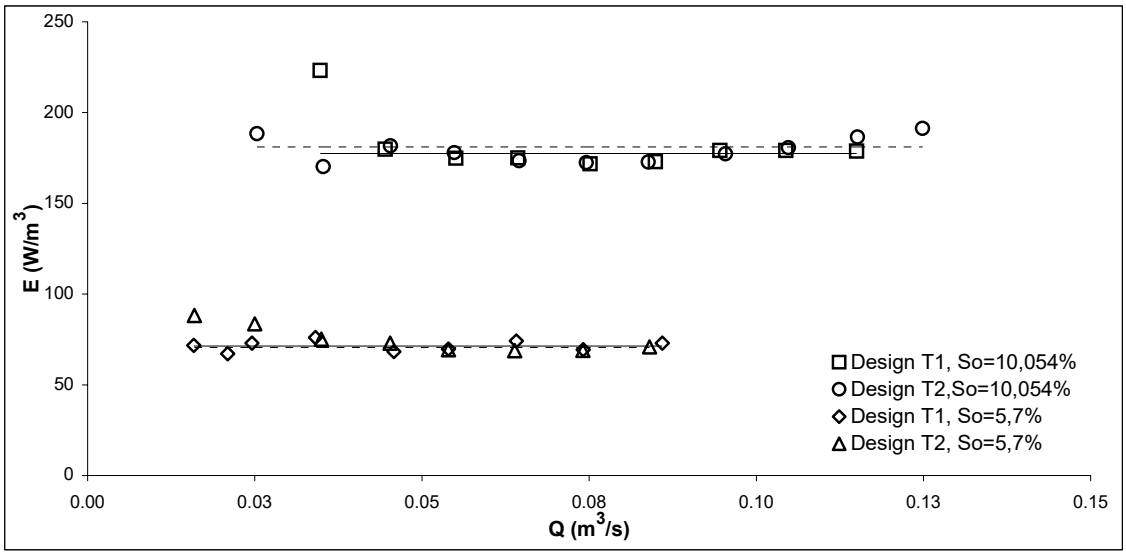

Fig. 16. Energy dissipation values versus circulating discharge in the model.

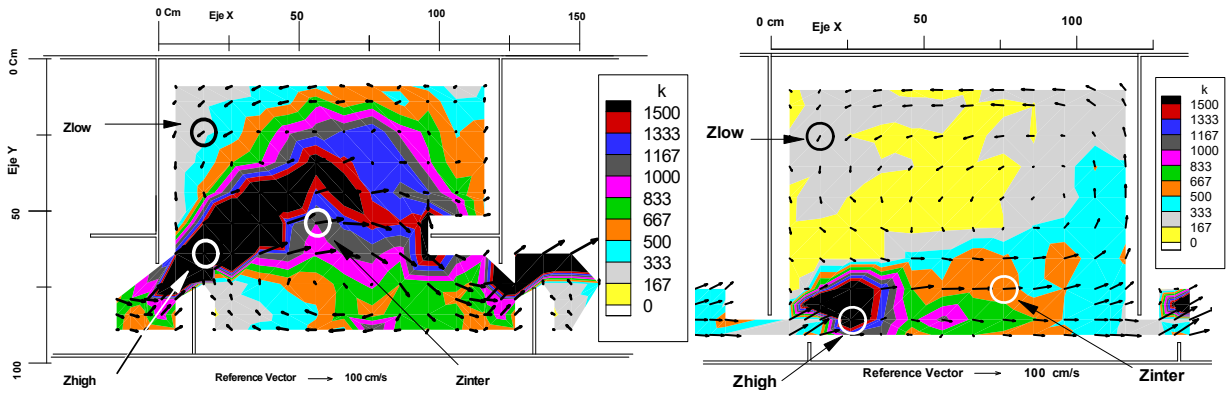

a) b)

Fig. 17. Contour lines of turbulent kinetic energy (cm^2/s^2) for a discharge of Q=0.085 m3/s. a) Design T1, So=10.054%, h=30 cm; b) Design T2, So=5.7%, h=60 cm .

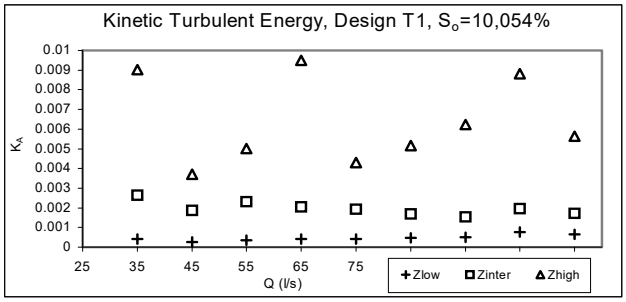

Fig. 18. Dimensionless turbulent kinetic energy, averaged on the vertical for design T1 and So=10.054%.

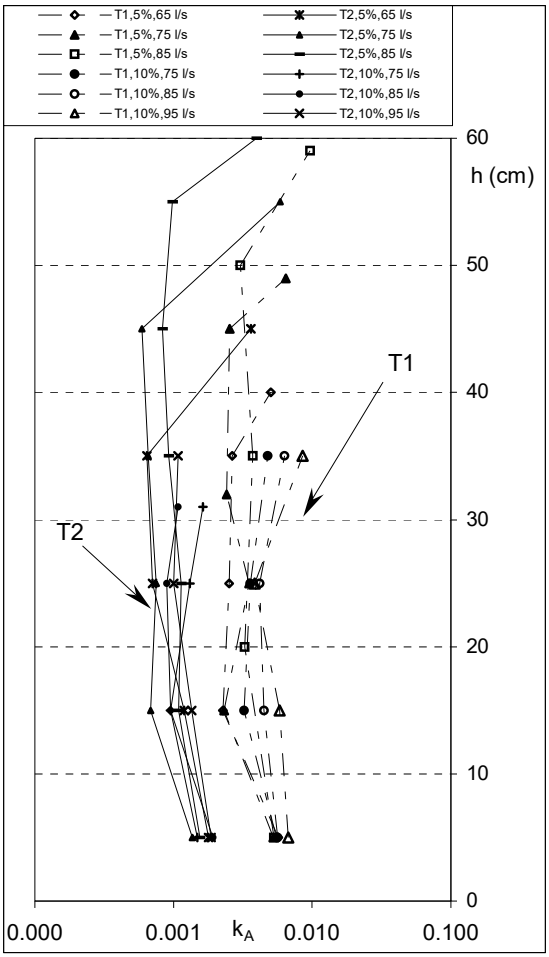

Fig. 19. Dimensionless turbulent kinetic energy versus depth (Z_{high}).

Table 1. Summary of present experiments.

Table 2. Summary of experimental results. All measurements are model data with b=0.16 m in the T1 design and b=0.15 m in the T2 design.

Table 3. Flow equations, relationship between dimensionless discharge and relative depths. In parentheses, correlation coefficent (r^2).

Table 4. Relationship between dimensionless discharge and relative depth with $Q^* = Q \Big/ \sqrt{g S_o b_o^5}$. In parentheses, correlation coefficent (r^2).

Table 5. Discharge-averaged mean velocity at slot

Table 6. Energy dissipation rate for fishway model and for standard prototype with a slot width b=0.305 m.

Table 7. Specific values of turbulent kinetic energy.

Fig. 1. Details of designs 6, 16 and 18, recommended for practical use by Rajaratnam *et al.* (1986, 1992).

Fig. 2. a) Dimension of the laboratory model of a vertical slot fishway. b and c) Details of T1 and T2 designs. d) Data point mesh in a parallel plane to the bed for T1 design and a slope of 10,054%.

Fig. 3. Cartesian positioner used to place the measurement gauges automatically over the experimental pools.

Fig. 4. Dimensionless relationship a) Q^A against Y_o/b, and b) Q* against Y_o/b.

Fig. 5. Dimensionless relationship discharge against depth in a standard prototype (b=0.305 m) for several designs.

Fig. 6. Relationship between characteristic depths, in the T2 design for S_0=5,7%.

Fig. 7. Contour lines of water free surface in the fishway model, for a discharge Q=0.065 m^3. a) Design T1, S_o=5,7%. b) Design T1, S_o=10,054%. c) Design T2, S_o=5,7%. d) Design T2, S_o=10,054%.

Fig. 8. Experimental depth values on a straight line linking two consecutive vertical slots, for discharge Q=0,065 m^3.

Fig. 9. Horizontal velocity fields, V_x-V_y in planes parallel to the bed for several experimental situations: a) Design T1, S=5,7%, Q=85 l/s, h=35 cm; b) Design T1, S=10,054%, Q=105 l/s, h=5 cm; c) Design T2, S=5,7%, Q=54 l/s, h=25 cm; d) Design T2, S=10,054%, Q=75 l/s, h=25 cm

Fig. 10. Flow patterns in pools: a) Design T1, S_o=5,7%; and S_o=10.054% with Q^A<2.75. b) Design T1, S_o=10.054% with Q^A>2.75. c) Design T2.

Fig. 11. Velocity fields, V_x-V_z in vertical planes parallel to longitudinal axis of fishway. a) T1 design, S_o=5,7%, Q=0,065 m^3, Y=72 cm b) T2 design, S_o=10,054%, Q=0,0746 m^3, Y=86 cm

Fig. 12. Vertical distributions of velocity values at some points for several discharge. a) T2 design, S_0=10,054% in: Pt. 1 x=76 cm, y=46 cm; Pt. 2 x=76 cm, y=11 cm; and Pt. 3 x=56 cm, y=86 cm. b) T1 design, S_o=5.7% in: Pt. 4 x=36 cm, y=12 cm; and Pt. 5 x=36 cm, y=62 cm.

Fig. 13. Velocity evolution against discharge at several experiemental data points. a) T1 design, S_o=10.054; b) T2 design, S_o=5.-7%.

Fig. 14. Values of the slot velocity against distance to the bed for several discharges. a) T1 design, So=5.7%; b) T2 design, So=10.054%.

Fig. 15. Depth average slot velocities versus discharge.

Fig. 16. Energy dissipation values versus circulating discharge in the model.

Fig. 17. Contour lines of turbulent kinetic energy (cm^2/s^2) for a discharge of Q=0.085 m3/s. a) Design T1, So=10.054%, h=30 cm; b) Design T2, So=5.7%, h=60 cm

Fig. 18. Dimensionless turbulent kinetic energy, averaged on the vertical for design T1 and So=10.054%.

Fig. 19. Dimensionless turbulent kinetic energy versus depth (Z_{high}).

***Keywords*: Fishways, vertical slot fishway, hydraulic models, open-channel flow, flow patterns, water velocity, water depth, energy dissipation, kinetic turbulent energy.**